

Supplemental Information for

Synthetically Tunable Polymers, Free Volume Element Size Distributions, and Dielectric Breakdown Field Strengths

Sebastian M. Fica-Contreras¹, Zongze Li², Abdullah Alamri³, Aaron P. Charnay¹, Junkun Pan¹, Chao Wu², Jeffrey R. Lockwood⁴, Omer Yassin⁴, Stuti Shukla⁴, Gregory Sotzing^{3,4*}, Yang Cao^{2*}, and Michael D. Fayer^{1*}

¹Department of Chemistry, Stanford University, Stanford, CA, 94305, USA

²Department of Electrical and Computer Engineering, University of Connecticut, Storrs, CT 06269, USA

³Institute of Materials Science, University of Connecticut, Storrs, CT 06269, United States

⁴Department of Chemistry, University of Connecticut, Storrs, CT, 06269, USA

E-mail: fayer@stanford.edu

E-mail: yang.cao@uconn.edu

E-mail: g.sotzing@uconn.edu

A. Structural determination of synthetic PEI samples.

1. Synthesis of 4-*tert*-butylaniline-PEI.

4,4-Bisphenol A Dianhydride (BisDA) (2.6 g, 5 mmol), *m*-phenylenediamine (0.52 g, 4.88 mmol), and 4-*tert*-butylaniline (0.036 g, 0.24 mmol) were placed in a 100 mL round bottom flask. 20 mL of *m*-cresol was then added to the reaction vessel and stirred overnight to form polyamic acid. After polyamic acid formation, the temperature was increased to 180 °C for 12 hours. The reaction was then cooled to room temperature, precipitated from methanol, and filtered. The final polymer was purified by Soxhlet extraction with methanol to remove residual *m*-cresol. Finally, the polymer was filtered and dried in a vacuum oven overnight at 140 °C. ¹H NMR (500 MHz, CDCl₃, ppm): δ = 7.89 (d, 1H), δ = 7.64(d, 1H), 7.58 (s, 1H) δ =7.51 (d,1H), δ = 7.42 (s, 1H), δ = 7.36 (m, 1H), δ = 7.32 (m, 1H), δ = 7.04 (d, 1H), δ = 6.82 (d, 1H), δ = 1.77 (s, 6H). Figure S2 shows the ¹HNMR for the synthesis of 4-*tert*-butylaniline-PEI.

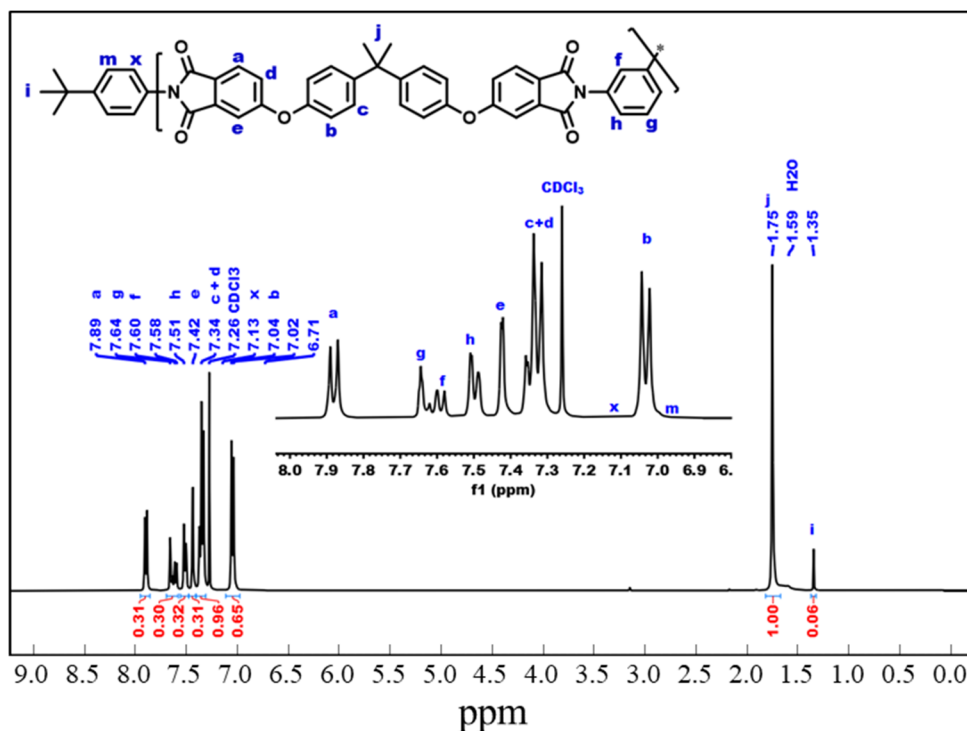


Figure S1. ¹H NMR spectrum of 4-*tert*-butylaniline-PEI in CDCl₃.

2. Synthesis of 2,4,6-tri-*tert*-butylaniline-PEI.

4,4-Bisphenol A Dianhydride (BisDA) (2.6 g, 5 mmol), *m*-phenylenediamine (0.52 g, 4.88 mmol), and 2,4,6-tri-*tert*-butylaniline (0.055 g, 0.21 mmol) were placed in a 100 mL round bottom flask. 20 mL of *m*-cresol was then added to the reaction vessel and stirred overnight to form polyamic acid. After polyamic acid formation, the temperature was increased to 180 °C for 12 hours. The reaction was then cooled to room temperature, precipitated from methanol, and filtered. The final polymer was purified by Soxhlet extraction using methanol to remove residual *m*-cresol. Finally, the polymer was filtered and dried in a vacuum oven overnight at 140 °C. ¹H NMR (500 MHz, CDCl₃, ppm): δ = 7.89 (d, 1H), δ = 7.64(d, 1H), 7.58 (s, 1H) δ =7.51 (d,1H), δ = 7.42 (s, 1H), δ = 7.36 (m, 1H), δ = 7.32 (m, 1H), δ = 7.04 (d, 1H), δ = 6.82 (d, 1H), δ = 1.77 (s, 6H), δ = 1.39 (s, 9H), δ = 1.35 (s, 9H). Figure S3 shows the ¹HNMR for the synthesis of 2,4,6-tri-*tert*-butylaniline-PEI

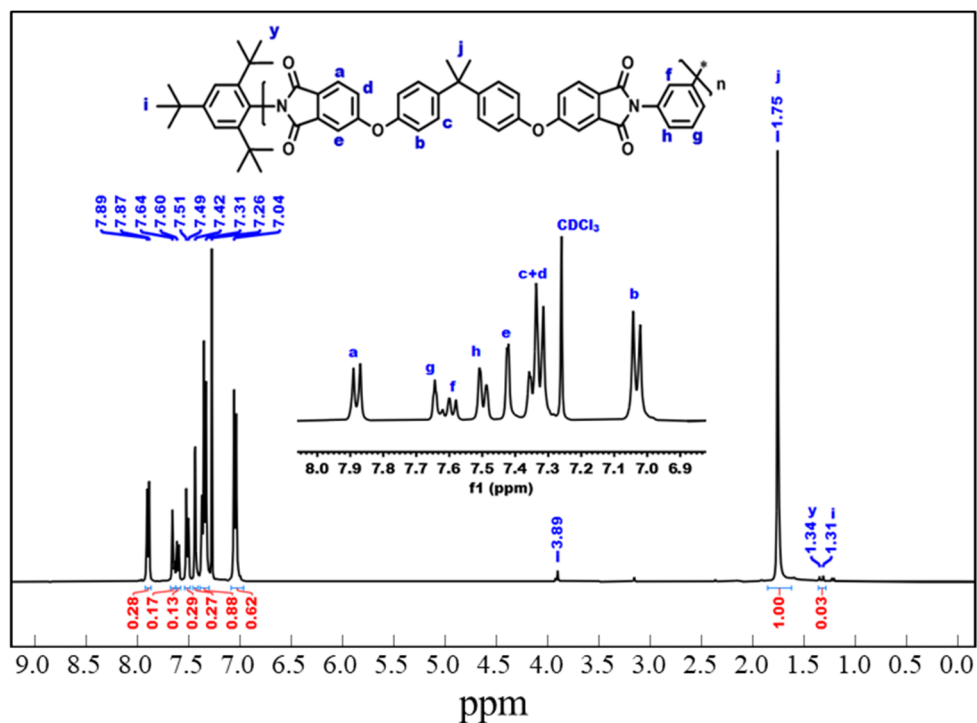


Figure S2. ¹H NMR spectrum of 2,4,6 tri-*tert*-butylaniline-PEI in CDCl₃.

3. Synthesis of 1-adamantylamine-PEI.

4,4-Bisphenol A Dianhydride (BisDA) (2.6 g, 5 mmol), *m*-phenylenediamine (0.52 g, 4.88 mmol), and 1-adamantylamine (0.036 g, 0.24 mmol) were placed in a 100 mL round bottom flask. 20 mL of *m*-cresol was then added to the reaction vessel and stirred overnight to form polyamic acid. After polyamic acid formation, the temperature was increased to 180 °C for 12 hours. The reaction was then cooled to room temperature and precipitated from methanol, filtered, and the final polymer was purified by Soxhlet extraction using methanol to remove residual *m*-cresol. Finally, the polymer was filtered and dried in a vacuum oven overnight at 140 °C. ¹H NMR (500 MHz, CDCl₃, ppm): δ = 7.89 (d, 1H), δ = 7.64(d, 1H), 7.58 (s, 1H) δ =7.51 (d,1H), δ = 7.42 (s, 1H), δ = 7.36 (m, 1H), δ = 7.32 (m, 1H), δ = 7.04 (d, 1H), δ = 6.82 (d, 1H), δ = 2.40 (s, 8H), δ = 2.14 (s, 8H), δ = 1.77 (s, 6H), δ = 1.35 (s, 9H). Figure S4 shows the ¹HNMR for the synthesis of 1-adamantylamine-PEI.

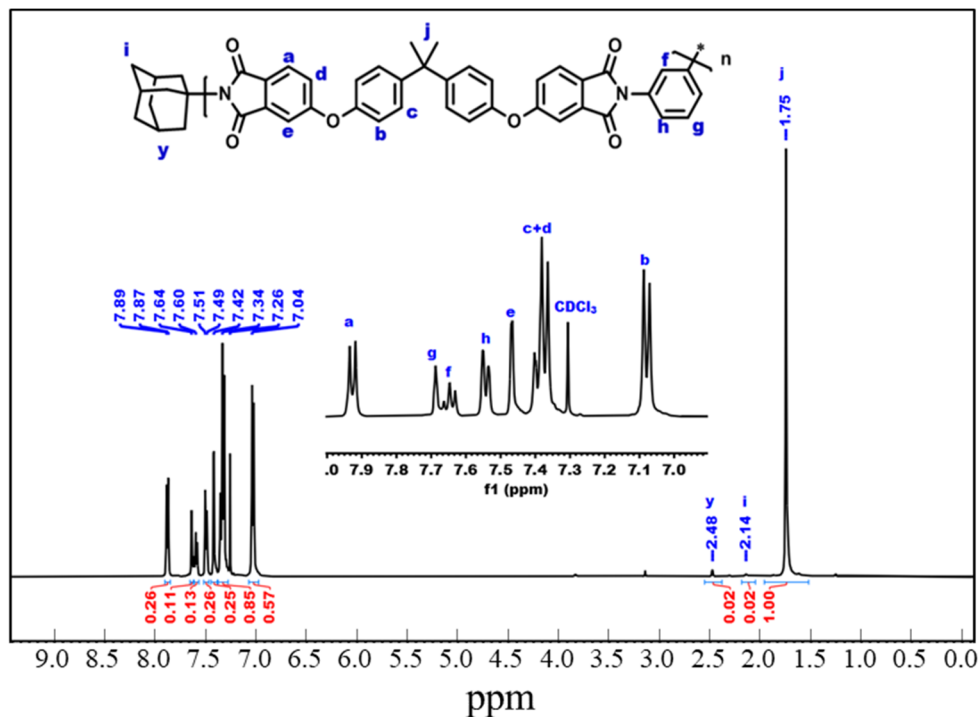


Figure S3. ¹H NMR spectrum of 1-adamantylamine-PEI in CDCl₃.

4. Synthesis of *p*-toluidine –PEI.

4,4-Bisphenol A Dianhydride (BisDA) (2.6 g, 5 mmol), *m*-phenylenediamine (0.52 g, 4.88 mmol), and *p*-toluidine (0.024 g, 0.22 mmol) were placed in a 100 mL round bottom flask. 20 mL of *m*-cresol was then added to the reaction vessel and stirred overnight to form polyamic acid. After polyamic acid formation, the temperature was increased to 180 °C for 12 hours. The reaction was then cooled to room temperature and precipitated from methanol, filtered, and the final polymer was purified by Soxhlet extraction using methanol to remove residual *m*-cresol. Finally, the polymer was filtered and dried in a vacuum oven overnight at 140 °C. ¹H NMR (500 MHz, CDCl₃, ppm): δ = 7.89 (d, 1H), δ = 7.64(d, 1H), 7.58 (s, 1H) δ =7.51 (d,1H), δ = 7.42 (s, 1H), δ = 7.36 (m, 1H), δ = 7.32 (m, 1H), δ = 7.04 (d, 1H), δ = 6.82 (d, 1H), δ = 2.40 (s, 6H), δ = 1.77 (s, 6H). Figure S4 shows the ¹HNMR for the synthesis of *p*-toluidine -PEI.

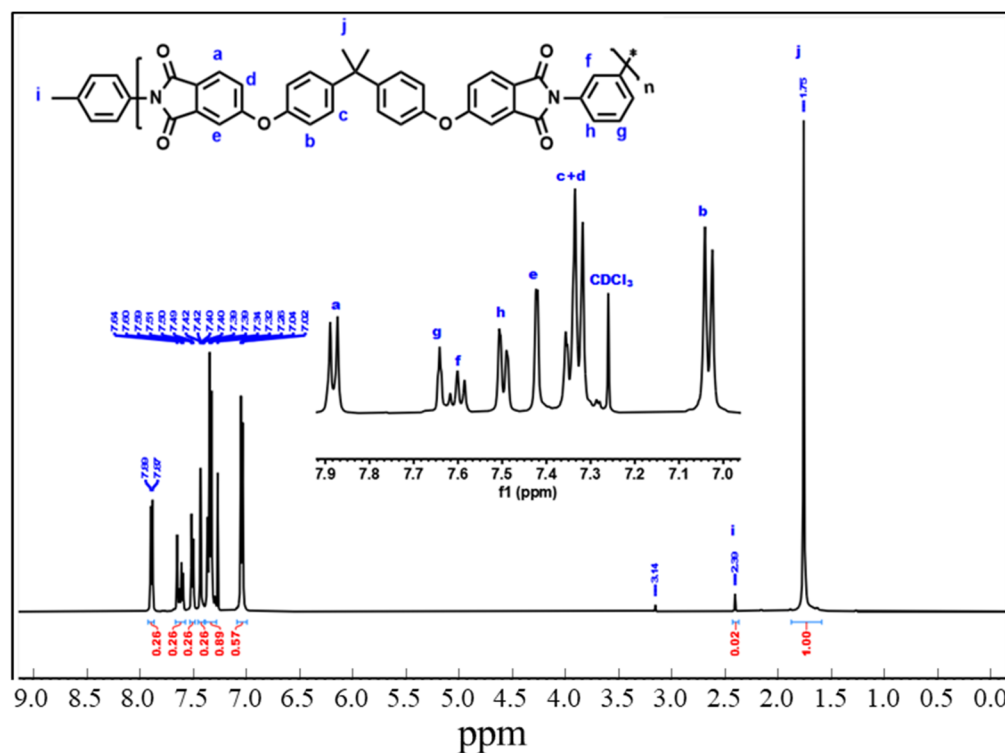


Figure S4. ¹H NMR spectrum of *p*-toluidine-PEI in CDCl₃.

B. Polymer characterization

1. Molecular weight determination

Gel Permeation Chromatography (GPC) was used to determine the molecular weight of all PEI samples. The polymers were dissolved in dimethylacetamide (DMAc) at a concentration of 0.25 weight %. Once fully dissolved, the solutions were filtered through a 45 μm syringe filter before injection into the instrument. The mobile phase used was also DMAc, and the instrument was calibrated using polystyrene (PS) or poly(methyl methacrylate) (PMMA) standards from PSS-Polymer Standards Service GmbH. The measured molecular weights are summarized in Table S1.

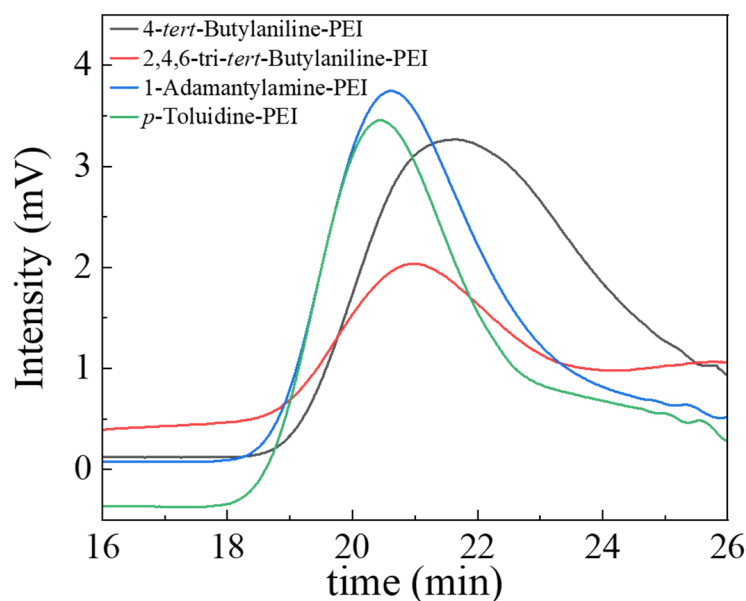


Figure S5. Gel permeation chromatographs for 4-*tert*-butylaniline-PEI, 2,4,6-tri-*tert*-butylaniline-PEI, 1-adamantylamine-PEI, and *p*-toluidine-PEI.

Table S1. Number-average molecular weight (M_n) and average molecular weight (M_w) of end capped PEI.

Polymer	M_n (Da)	M_w (Da)	PDI	M_n (NMR) (Da)
<i>p</i> -Toluidine-PEI	29,900	63,687	2.13	29,600
4- <i>tert</i> -Butylaniline-PEI	26,500	48,060	1.78	25,491
1-Adamantylamine-PEI	29,620	57,466	1.94	27,100
2,4,6-tri- <i>tert</i> -Butylaniline-PEI	29,300	62,713	2.13	26,400

2. Thermal characterization

The glass transition and thermal degradation temperatures of PEI were measured using thermo-gravimetric Analysis (TGA) and Differential Scanning Calorimetry (DSC). Figure S6 shows the TGA curves of synthetic PEI with different end groups. Figure S7 shows the DSC curves for the same set of synthetic PEI samples. The glass transition temperatures of the end capped PEI samples show no significant differences.

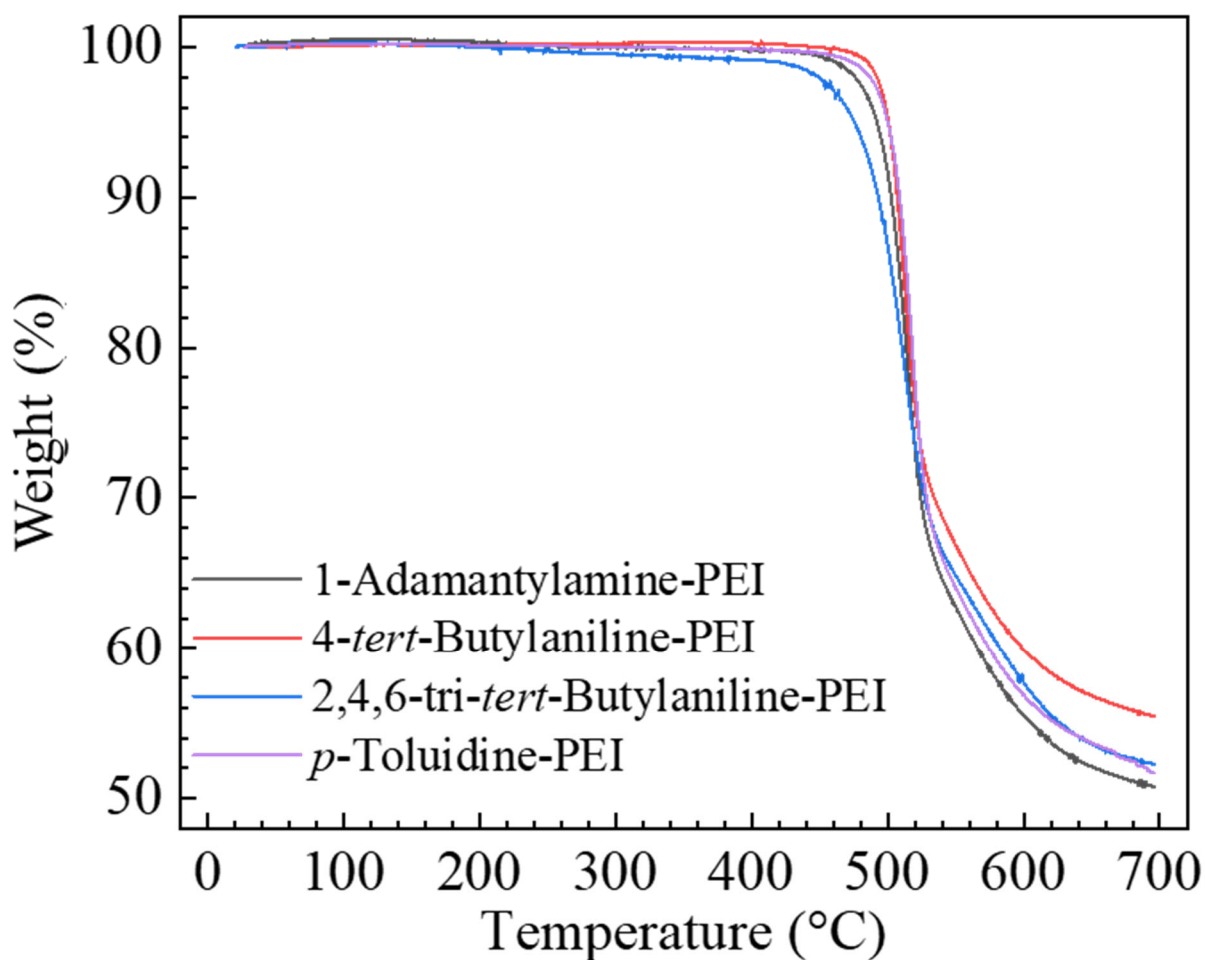


Figure S6. TGA curves for PEI with different end groups.

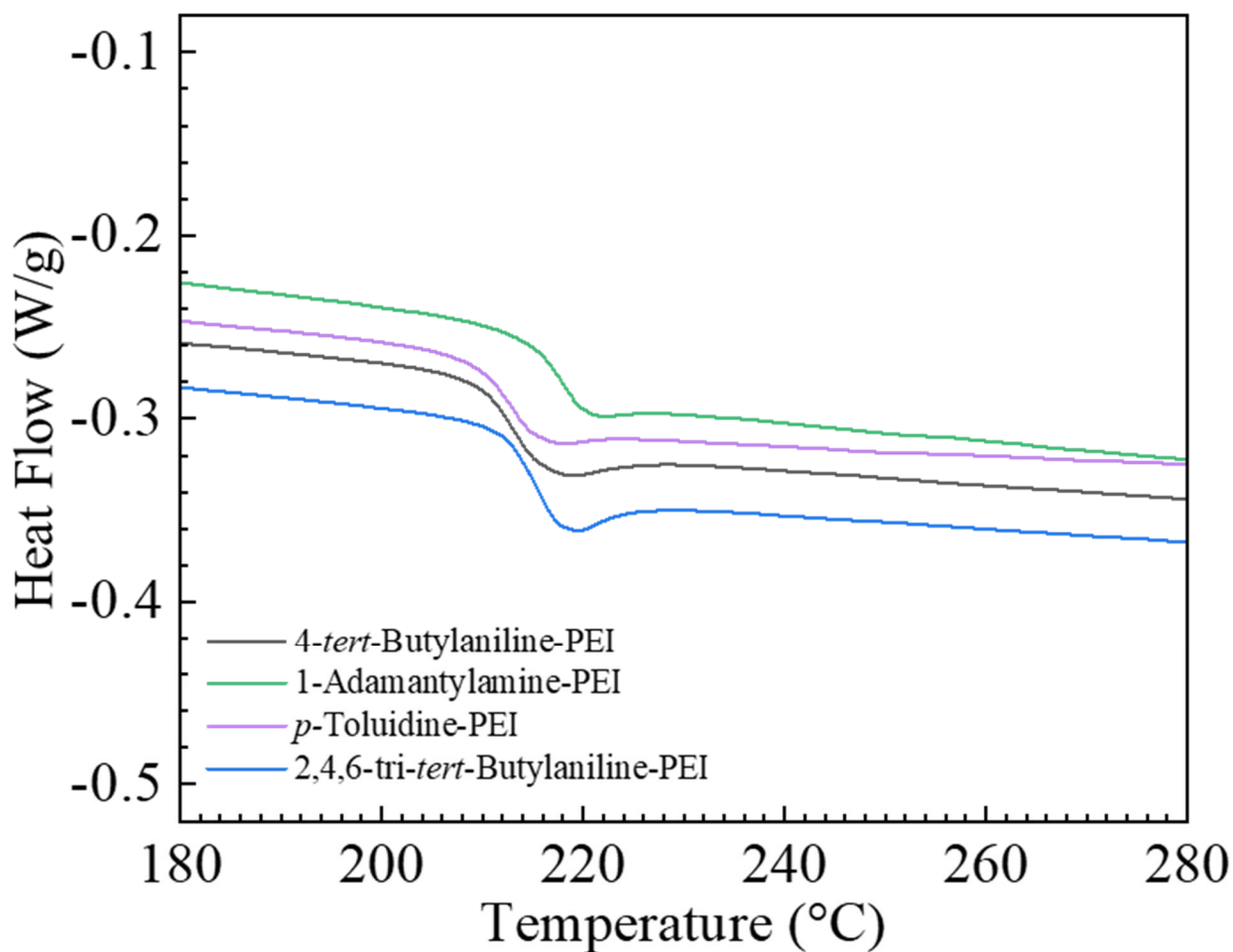


Figure S7. DSC curves for PEI with different end groups.

C. Electrical characterization

1. Dielectric constant determination

4-*tert*-Butylaniline-PEI, 2,4,6-tri-*tert*-butylaniline-PEI, and 1-adamantylamine-PEI displayed dielectric constant values between 3.1 to 3.3 and remained virtually unchanged with temperature. These values are consistent with reports of the dielectric constant of PEI in the literature. The similarities across films demonstrate that the identity of the endcap does not significantly influence the dielectric constant properties of PEI. The dielectric constants of only these three

polymers were measured because these were the same films for which a breakdown measurement was possible.

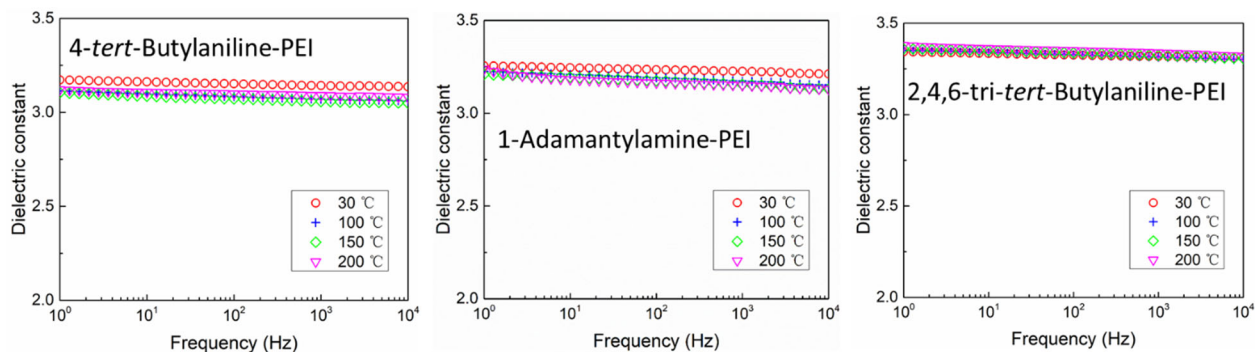


Figure S8. The dielectric constant for PEI end cap with 4-*tert*-butylaniline, 2,4,6-tri-*tert*-butylaniline, and 1-adamantylamine at different temperatures.

D. Drying PEI films for ultrafast spectroscopic measurements.

The end capped PEI films were dried in a vacuum oven at <100 mTorr and in gradual temperature increments. The drying cycle was started with 1 day at 100 °C, followed by 1 day at 120 °C, 3 days at 140 °C, and finally 1 day at 160 °C. A gradual increase in temperature was preferred to avoid the formation of bubbles on the surface of the membranes. NMR was used to ensure the films were dry. Fig. S9 shows a sample NMR spectrum of a PEI film with solvent to illustrate the positions of the peaks. Fig. S10 shows the NMR spectra of the end capped membranes after drying to show that they were all free of any residual solvent.

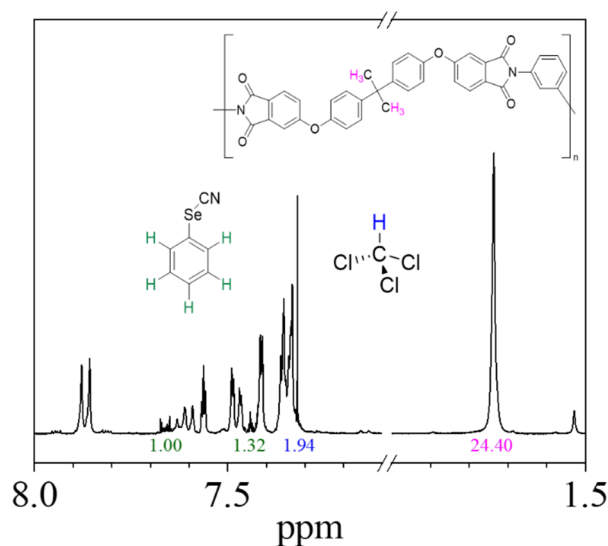


Figure S9. ^1H NMR spectrum in CD_2Cl_2 of a PEI membrane. This membrane contains chloroform on purpose to show an example of a wet film NMR spectrum. The relevant peaks and atoms are color coded. This membrane displays signals for PhSeCN, chloroform and PEI. The numerical values under the peaks indicate the relevant areas used for quantification of the solvent, polymer, and probe.

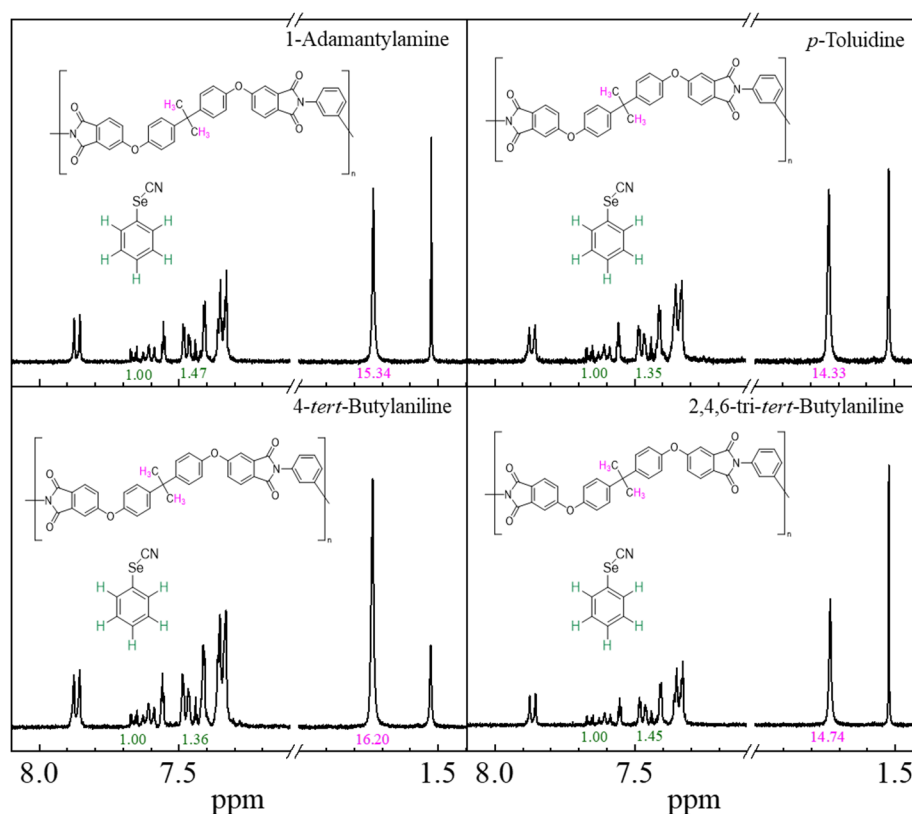


Figure S10. ^1H NMR spectra in CD_2Cl_2 of end capped PEI films. The relevant peaks and atoms are color coded. These spectra display no signal from chloroform, which demonstrates that the membranes are completely dry and free of residual solvent. The numerical values under the peaks indicate the relevant areas used for quantification of the solvent, polymer, and probe.

Linear absorption spectra of PhSeCN in five PEI films

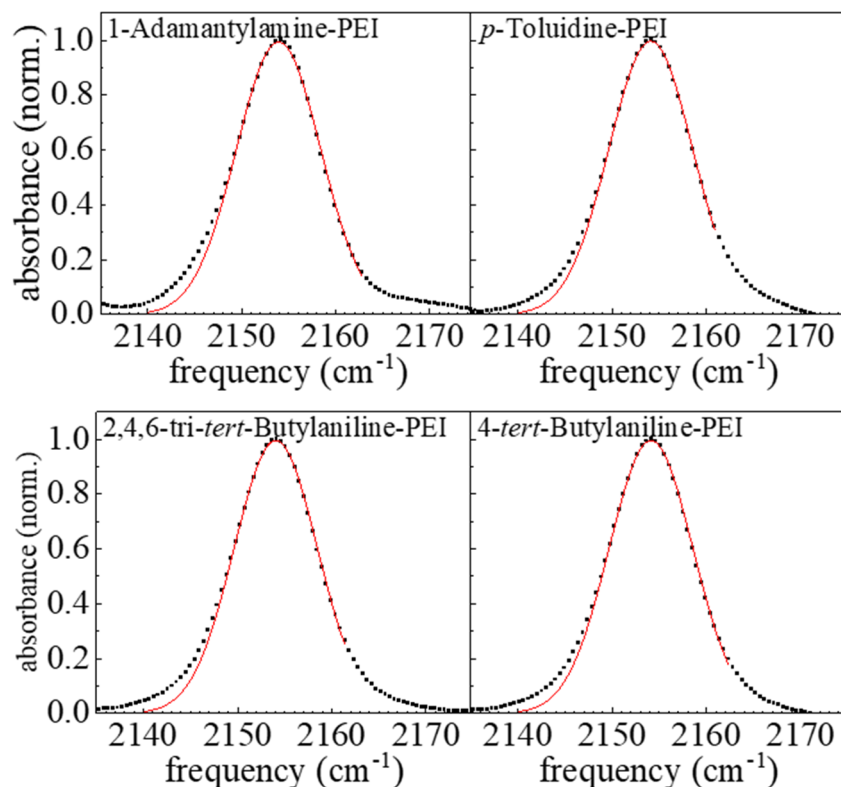


Figure S11, Linear absorption spectra of symmetric CN stretch vibration of PhSeCN in end capped PEI films. The solid lines represent a Gaussian fit to the high frequency regime data, extended to the low frequency regime. These fits show that a Gaussian lineshape fails to capture the shape of the absorption spectrum at low frequency. This effect has been observed before with poly(methyl methacrylate) and polystyrene and it is directly related to a non-Gaussian distribution of FVE radii in the membranes. The parameters that describe the fits are summarized in Table S2.

Table S2. Parameters that describe the Gaussian fit to the linear absorption spectrum of the symmetric CN stretch of PhSeCN in end capped PEI membranes.

Polymer	Center (cm ⁻¹)	FWHM (cm ⁻¹)
<i>p</i> -Toluidine-PEI	2154.1 ± 0.1	10.5 ± 0.1
4- <i>tert</i> -Butylaniline-PEI	2154.1 ± 0.1	10.4 ± 0.1
1-Adamantylamine-PEI	2153.9 ± 0.1	10.6 ± 0.1
2,4,6-tri- <i>tert</i> -Butylaniline-PEI	2154.1 ± 0.1	10.4 ± 0.1

E. Orientational Dynamics

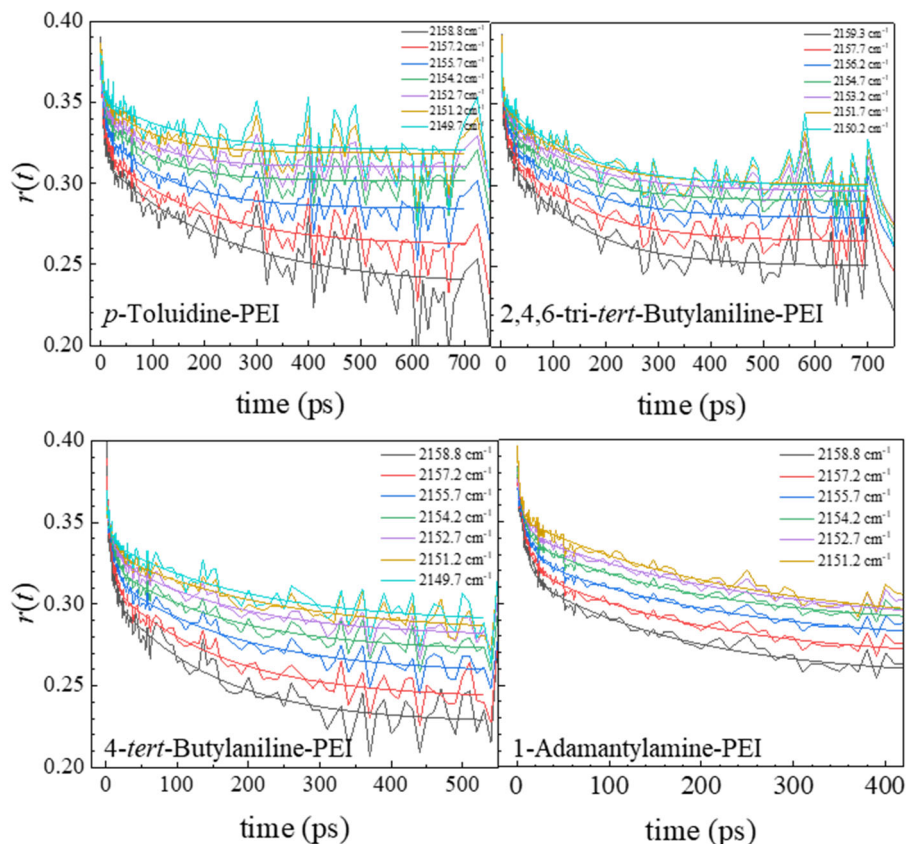


Figure S12. Frequency dependent orientational dynamics curves of PhSeCN end capped PEI films. All data sets display a strong frequency dependence of the orientational dynamics, with a tendency to converge at low frequency. All curves are best characterized by a biexponential decay to a non-zero, frequency dependent, final static offset. The curves were also fitted with the wobbling-in-a-cone equation shown in the main text to extract frequency dependent FVE radii. The parameters that describe both the biexponential and wobbling-in-a-cone fits are presented in Tables S3-10.

Table S3. Parameterization of orientational dynamics curves of PhSeCN in *p*-toluidine-PEI membranes using the wobbling-in-a-cone model.

Frequency (cm ⁻¹)	S_0	S_1	τ_1 (ps)	S_2	τ_2 (ps)
2158.8	0.86 ± 0.01	0.86 ± 0.05	29.6 ± 10.9	0.86 ± 0.03	203 ± 210
2157.2	0.94 ± 0.01	0.86 ± 0.01	5.7 ± 1.2	0.82 ± 0.01	142 ± 31
2155.7	0.94 ± 0.01	0.89 ± 0.01	5.3 ± 1.5	0.86 ± 0.01	112 ± 26
2154.2	0.94 ± 0.01	0.91 ± 0.01	4.5 ± 1.6	0.88 ± 0.01	95 ± 23
2152.7	0.93 ± 0.01	0.94 ± 0.01	3.6 ± 1.9	0.89 ± 0.01	95 ± 24
2151.2	0.96 ± 0.01	0.91 ± 0.01	3.5 ± 1.3	0.90 ± 0.01	96 ± 28
2149.7	0.95 ± 0.01	0.93 ± 0.01	2.8 ± 1.4	0.91 ± 0.01	119 ± 39

Table S4. Parameterization of orientational dynamics curves of PhSeCN in 4-*tert*-butylaniline-PEI membranes using the wobbling-in-a-cone model.

Frequency (cm ⁻¹)	S_0	S_1	τ_1 (ps)	S_2	τ_2 (ps)
2158.8	0.99 ± 0.01	0.78 ± 0.01	5.4 ± 0.7	0.74 ± 0.01	143 ± 18
2157.2	0.97 ± 0.01	0.81 ± 0.01	6.3 ± 0.6	0.77 ± 0.01	155 ± 17
2155.7	0.94 ± 0.01	0.85 ± 0.01	8.3 ± 0.9	0.81 ± 0.01	178 ± 23
2154.2	0.93 ± 0.01	0.87 ± 0.01	7.9 ± 0.9	0.83 ± 0.01	168 ± 22
2152.7	0.92 ± 0.01	0.90 ± 0.01	8.4 ± 1.3	0.85 ± 0.01	174 ± 25
2151.2	0.91 ± 0.01	0.90 ± 0.01	9.4 ± 1.7	0.85 ± 0.01	226 ± 47

Table S5. Parameterization of orientational dynamics curves of PhSeCN in 1-adamantylamine-PEI membranes using the wobbling-in-a-cone model.

Frequency (cm ⁻¹)	S_0	S_1	τ_1 (ps)	S_2	τ_2 (ps)
2158.8	0.96 ± 0.004	0.83 ± 0.006	8.1 ± 0.7	0.80 ± 0.01	174 ± 25
2157.2	0.95 ± 0.003	0.86 ± 0.005	9.6 ± 0.7	0.82 ± 0.01	194 ± 29
2155.7	0.93 ± 0.003	0.88 ± 0.005	10.8 ± 0.9	0.83 ± 0.01	221 ± 40
2154.2	0.96 ± 0.003	0.89 ± 0.004	7.4 ± 0.7	0.84 ± 0.01	191 ± 27
2152.7	0.95 ± 0.004	0.91 ± 0.004	7.8 ± 0.9	0.83 ± 0.01	254 ± 49
2151.2	0.99 ± 0.008	0.88 ± 0.006	3.3 ± 0.4	0.81 ± 0.01	240 ± 39

Table S6. Parameterization of orientational dynamics curves of PhSeCN in 2,4,6-tri-*tert*-butylaniline-PEI membranes using the wobbling-in-a-cone model.

Frequency (cm ⁻¹)	S_0	S_1	τ_1 (ps)	S_2	τ_2 (ps)
2159.3	0.96 ± 0.01	0.85 ± 0.01	4.9 ± 0.7	0.77 ± 0.01	129 ± 16
2157.7	0.93 ± 0.01	0.88 ± 0.01	7.8 ± 1.2	0.81 ± 0.01	143 ± 22
2156.2	0.93 ± 0.01	0.89 ± 0.01	8.2 ± 1.3	0.84 ± 0.01	143 ± 23
2154.7	0.94 ± 0.01	0.91 ± 0.01	6.6 ± 1.1	0.85 ± 0.01	134 ± 21
2153.2	0.92 ± 0.01	0.92 ± 0.01	8.3 ± 1.7	0.86 ± 0.01	175 ± 36
2151.7	0.99 ± 0.01	0.88 ± 0.01	2.9 ± 0.5	0.85 ± 0.01	146 ± 21
2150.2	0.98 ± 0.02	0.89 ± 0.02	1.4 ± 0.4	0.84 ± 0.01	171 ± 27

Table S7. Parameterization of orientational dynamics curves of PhSeCN in *p*-toluidine-PEI membranes using a biexponential functional fit.

Frequency (cm ⁻¹)	A ₁	t ₁ (ps)	A ₂	t ₂ (ps)	y ₀
2158.8	0.069 ± 0.004	5.2 ± 0.8	0.071 ± 0.004	166 ± 32	0.248 ± 0.005
2157.2	0.050 ± 0.004	5.4 ± 0.9	0.057 ± 0.003	132 ± 22	0.268 ± 0.003
2155.7	0.040 ± 0.003	5.1 ± 1.0	0.048 ± 0.002	107 ± 17	0.287 ± 0.002
2154.2	0.032 ± 0.003	4.3 ± 1.1	0.042 ± 0.002	90 ± 14	0.303 ± 0.001
2152.7	0.023 ± 0.004	3.4 ± 1.3	0.038 ± 0.002	88 ± 15	0.311 ± 0.002
2151.2	0.033 ± 0.004	3.3 ± 1.1	0.033 ± 0.003	87 ± 19	0.320 ± 0.002
2149.7	0.026 ± 0.006	2.7 ± 1.4	0.030 ± 0.003	104 ± 31	0.325 ± 0.002

Table S8. Parameterization of orientational dynamics curves of PhSeCN in 4-*tert*-butylaniline-PEI membranes using a biexponential functional fit.

Frequency (cm ⁻¹)	A ₁	t ₁ (ps)	A ₂	t ₂ (ps)	y ₀
2158.8	0.088 ± 0.004	5.8 ± 0.6	0.086 ± 0.004	175 ± 27	0.220 ± 0.005
2157.2	0.073 ± 0.003	6.4 ± 0.6	0.073 ± 0.003	165 ± 21	0.240 ± 0.003
2155.7	0.057 ± 0.003	8.3 ± 0.9	0.062 ± 0.003	189 ± 30	0.256 ± 0.004
2154.2	0.049 ± 0.003	7.9 ± 0.9	0.054 ± 0.002	175 ± 28	0.270 ± 0.003
2152.7	0.038 ± 0.002	8.8 ± 1.2	0.052 ± 0.003	198 ± 36	0.277 ± 0.004
2151.2	0.030 ± 0.003	9.1 ± 1.8	0.049 ± 0.003	197 ± 42	0.285 ± 0.004

Table S9. Parameterization of orientational dynamics curves of PhSeCN in 1-adamantylamine-PEI membranes using a biexponential functional fit.

Frequency (cm ⁻¹)	A ₁	t ₁ (ps)	A ₂	t ₂ (ps)	y ₀
2158.8	0.064 ± 0.002	7.7 ± 0.6	0.064 ± 0.002	162 ± 22	0.256 ± 0.003
2157.2	0.054 ± 0.002	9.2 ± 0.7	0.058 ± 0.002	185 ± 27	0.267 ± 0.003
2155.7	0.044 ± 0.002	10.5 ± 0.9	0.054 ± 0.003	213 ± 36	0.276 ± 0.004
2154.2	0.043 ± 0.002	7.1 ± 0.6	0.053 ± 0.002	183 ± 25	0.287 ± 0.003
2152.7	0.035 ± 0.002	7.5 ± 0.9	0.059 ± 0.004	242 ± 46	0.286 ± 0.005
2151.2	0.050 ± 0.003	3.0 ± 0.4	0.065 ± 0.004	222 ± 34	0.288 ± 0.005

Table S10. Parameterization of orientational dynamics curves of PhSeCN in 2,4,6-tri-*tert*-butylaniline-PEI membranes using a biexponential functional fit.

Frequency (cm ⁻¹)	A ₁	t ₁ (ps)	A ₂	t ₂ (ps)	y ₀
2159.3	0.059 ± 0.003	4.6 ± 0.6	0.073 ± 0.002	124 ± 14	0.252 ± 0.002
2157.7	0.045 ± 0.003	7.4 ± 1.0	0.062 ± 0.002	138 ± 19	0.266 ± 0.002
2156.2	0.040 ± 0.003	7.6 ± 1.1	0.054 ± 0.002	134 ± 19	0.280 ± 0.002
2154.7	0.035 ± 0.002	6.0 ± 1.0	0.050 ± 0.002	124 ± 16	0.290 ± 0.002
2153.2	0.024 ± 0.003	7.7 ± 1.8	0.048 ± 0.002	144 ± 23	0.295 ± 0.002
2151.7	0.046 ± 0.004	2.7 ± 0.5	0.050 ± 0.002	137 ± 17	0.299 ± 0.002
2150.2	0.043 ± 0.008	1.3 ± 0.4	0.054 ± 0.002	156 ± 21	0.298 ± 0.003

F. FVE Radius Probability Distribution (RPD) Curves.

The maximum entropy calculations are required to simultaneously fit the frequency-dependent radii data and the probe's absorption spectrum, which ensures a highly restricted resulting distribution of FVE radii. The calculations reproduce both the frequency-dependent FVE radii and the FT-IR spectrum with excellent agreement. The fits are shown below in Figs. S13 -16 for the end capped PEI membranes.

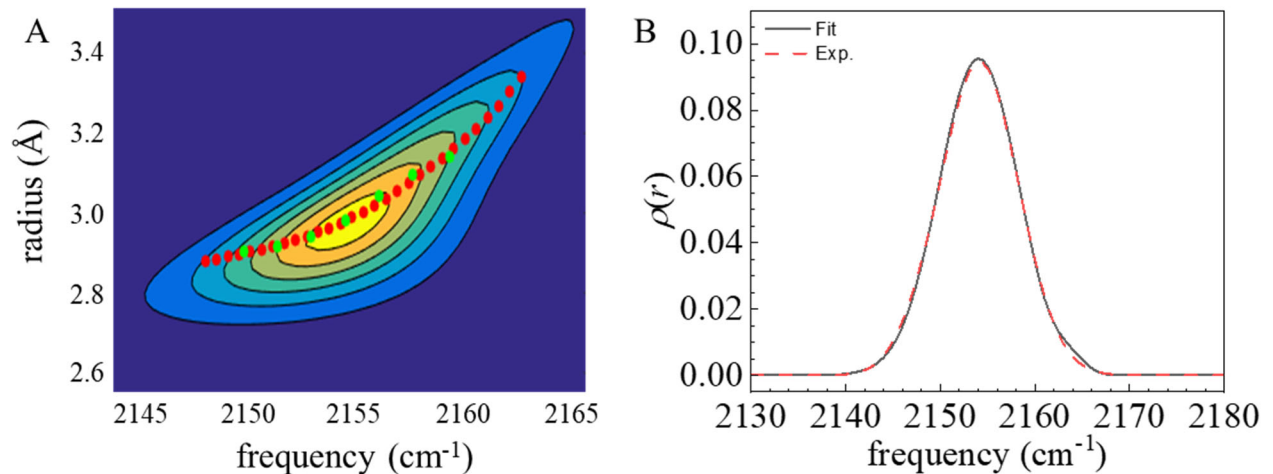


Figure S13. Results of the maximum entropy calculation for the FVE size distribution of 4-*tert*-butylaniline-PEI. (A) Contour plot of the joint probability distributions of FVE radius and probe frequency, $\rho(\omega, r)$. The green points are the measured radii vs frequency and the dotted red curve is the calculated radii vs frequency. (B) The experimental FT-IR spectrum (red dashed curve) and the calculated spectrum show quantitative agreement.

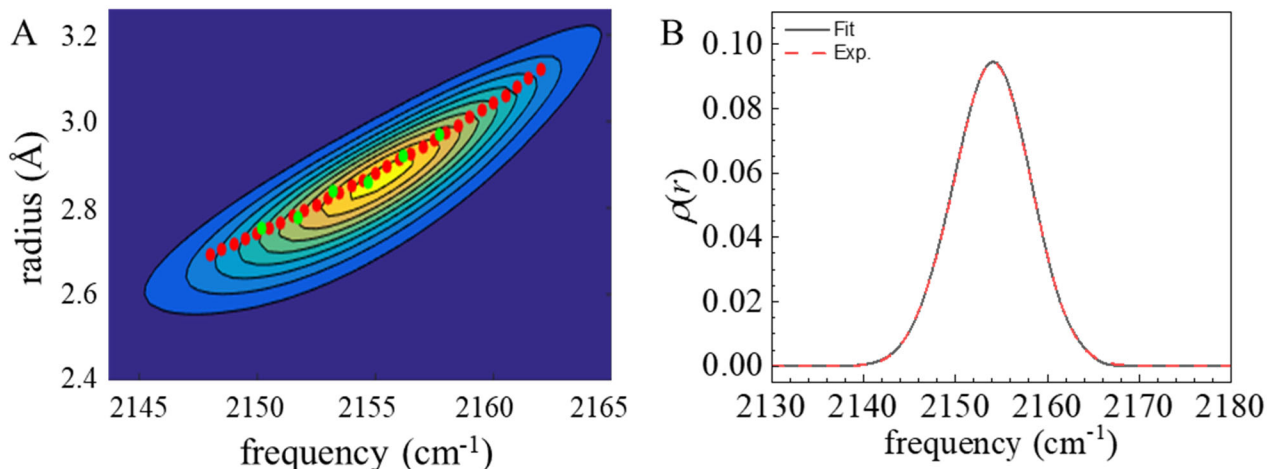


Figure S14. Results of the maximum entropy calculation for the FVE size distribution of 2,4,6-tri-*tert*-butylaniline-PEI. (A) Contour plot of the joint probability distributions of FVE radius and probe frequency, $\rho(\omega,r)$. The green points are the measured radii vs frequency and the dotted red curve is the calculated radii vs frequency. (B) The experimental FT-IR spectrum (red dashed curve) and the calculated spectrum show quantitative agreement.

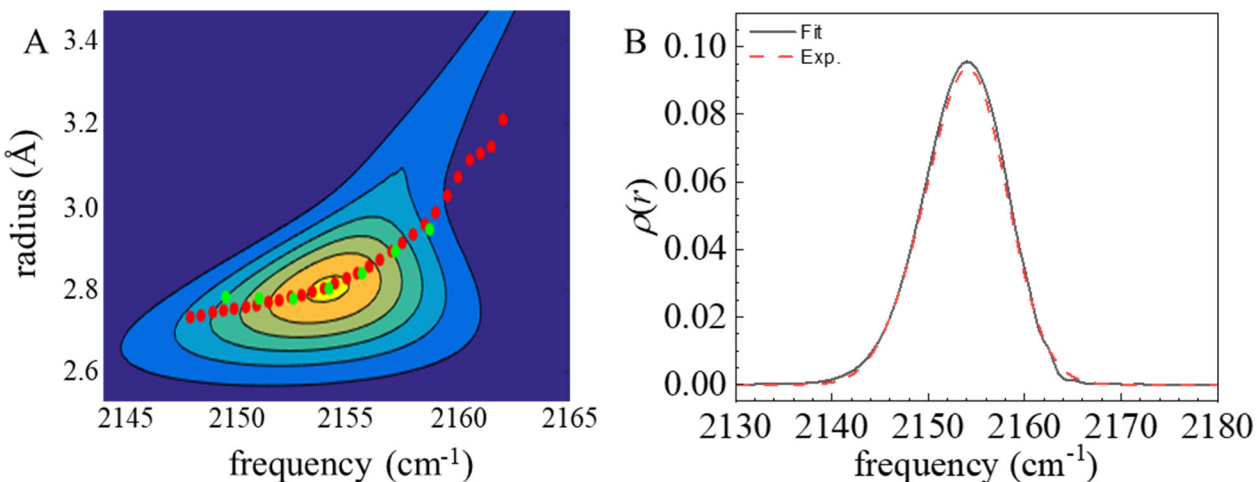


Figure S15. Results of the maximum entropy calculation for the FVE size distribution of 1-adamantylamine-PEI. (A) Contour plot of the joint probability distributions of FVE radius and probe frequency, $\rho(\omega,r)$. The green points are the measured radii vs frequency and the dotted red curve is the calculated radii vs frequency. (B) The experimental FT-IR spectrum (red dashed curve) and the calculated spectrum show quantitative agreement.

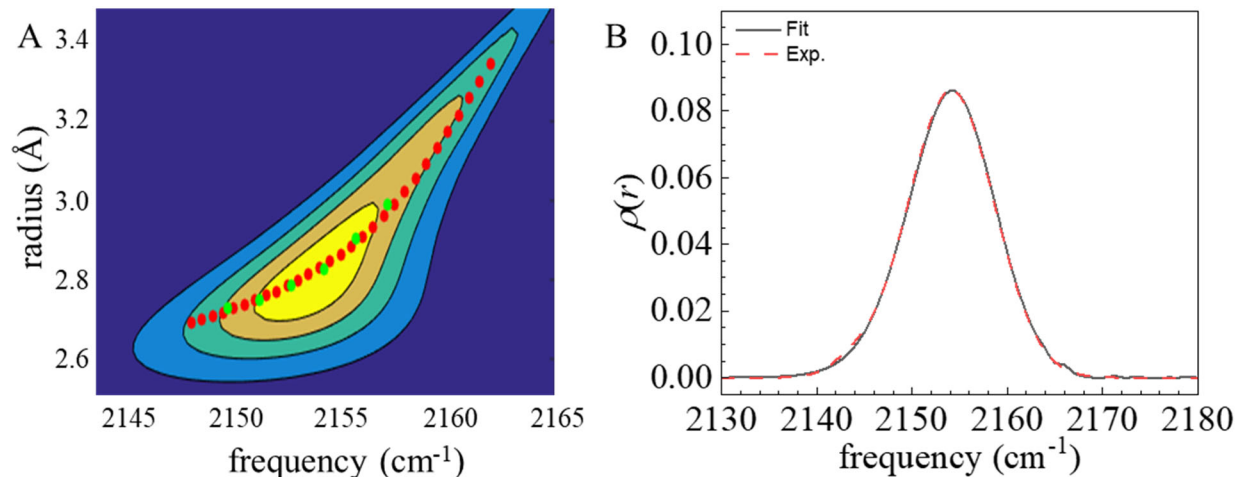


Figure S16. Results of the maximum entropy calculation for the FVE size distribution of *p*-toluidine-PEI. (A) Contour plot of the joint probability distributions of FVE radius and probe frequency, $\rho(\omega, r)$. The green points are the measured radii vs frequency and the dotted red curve is the calculated radii vs frequency. (B) The experimental FT-IR spectrum (red dashed curve) and the calculated spectrum show quantitative agreement.

G. Breakdown field measurements.

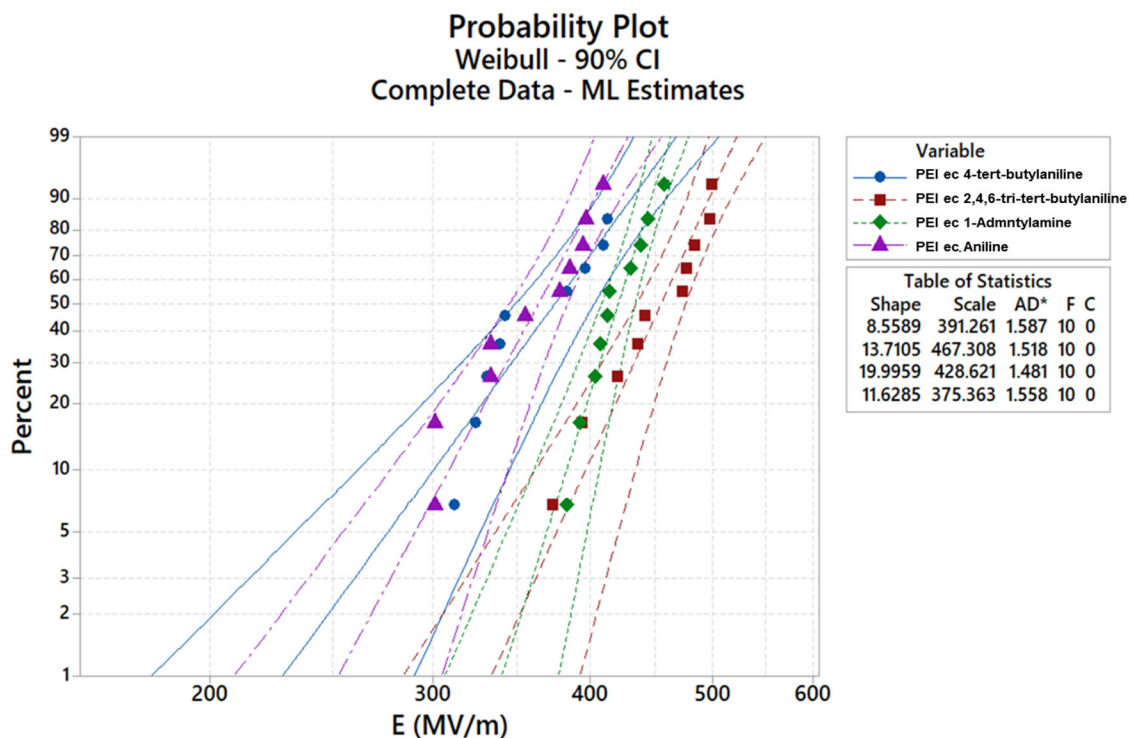


Figure S17. Weibull distribution of the breakdown strength for 4 types of PEI membranes.